European Journal of Agronomy 99 (2018) 92–105

Contents lists available at ScienceDirect

European Journal of Agronomy

journal homepage: www.elsevier.com/locate/eja

A model library to simulate grapevine growth and development: software implementation, sensitivity analysis and field level application

L. Leolini[a,*], S. Bregaglio[b], M. Moriondo[c], M.C. Ramos[d], M. Bindi[a], F. Ginaldi[b]

[a] DISPAA, University of Florence, Piazzale delle Cascine 18, 50144, Florence, Italy
[b] CREA - Council for Agricultural Research and Economics, Research Centre for Agriculture and Environment, via di Corticella 133, 40128, Bologna, Italy
[c] CNR-IBIMET, Via G. Caproni 8, 50145, Florence, Italy
[d] Department of Environment and Soil Science-Agrotecnio, University of Lleida, Alcalde Rovira Roure, 191, E-25198, Lleida, Spain

ARTICLE INFO

Keywords:
BioMA platform
Chardonnay
Latin hypercube sampling
Simplex optimization
Sobol' total order
Vineyard

ABSTRACT

Simulation modelling applied to grapevine is a promising tool to unravel the tight interactions between agricultural management and pedo-climatic conditions, and their impact on yield variability. This is an urgent need in current conditions, and in light of climate change, which is expected to deeply affect the performances of vine cropping systems. Here we present a BioMA software component (UNIFI.GrapeML), which is a model library of grapevine physiological processes. We used it to develop a new grapevine model considering the impact of soil water availability on yield, selecting a Spanish vineyard as case study (Chardonnay variety). We inspected its behavior with sensitivity analysis techniques, selecting the most relevant parameters to calibrate for matching reference data. The accuracy in reproducing phenology (average Pearson $\bar{r} = 0.57$), soil water content ($\bar{r} = 0.70$) and yield ($r = 0.59$) proved its capability to respond to weather variability, and the efficiency of BioMA software architecture in developing agricultural models.

Software availability

BioMA component nameUNIFI.GrapeML

DevelopersLuisa Leolini, Fabrizio Ginaldi, Simone Bregaglio

Availability and online documentationUNIFI.GrapeML is available as Software Development Kit (SDK) on http://www.biomamodelling.org/Components/. The SDK contains a help file with the documentation of algorithms and models, and two sample applications showing how to use UNIFI.GrapeML component as single software unit and in a modelling solution. UNIFI.GrapeML is released as C# libraries compiled for the NET 4.5 platform.

1. Introduction

Grapevine (*Vitis vinifera* L.) is the top cash crop worldwide (Williams and Ayars, 2005), being cultivated on 7.5 million hectares in 2015 (OIV, 2017) with a total production of nearly 77 Mt (FAOSTAT, 2016). The resulting global wine production remained quite stable under the 21st century, ranging between 257 mhl (millions of hectolitres) in 2002 to 274 mh l in 2015 (OIV, 2017), with the European Mediterranean region contributing to a quarter of total wine production, followed by South America (29.1 mhl), United States (22.1 mhl), Australia (12.0 mh l), and China (11.0 mh l).

The qualitative and quantitative performances of grapevine production systems are known to be largely affected by the complex interactions among environmental drivers (Jones et al., 2005; Ramos et al., 2008; Seguin, 1988), grapevine varieties (Huglin and Schneider, 1998; Lavee and May, 1997) and soil conditions (Seguin, 1986; Van Leeuwen and Seguin, 1994), including water and nutrients dynamics (Costantini and Bucelli, 2014). The evidence of global warming is thus posing a concrete threat to the economy of the three top producing countries - Italy, France and Spain - as their uppermost wine regions are placed in very sensitive areas to climate change (Gao and Giorgi, 2008), whose impacts are expected to affect especially the southernmost European areas (Hannah et al., 2013; Jones et al., 2005; Leolini et al., 2017; Moriondo et al., 2013).

Available studies, indeed, evidenced that climate change already impacted on vine development, yield and quality by moving in advance phenological stages (Duchêne and Schneider, 2005; Jones and Davis, 2000; Tomasi et al., 2011; Van Leeuwen and Darriet, 2016), increasing sugar content (Duchêne and Schneider, 2005; Van Leeuwen and Darriet, 2016) and yield in regions where low temperatures represent a limiting factor for production (Bock et al., 2013). However, the general picture of the process is not univocally defined as there is a strong interaction between phenology and grapevine performances in terms of

* Corresponding author.
E-mail address: luisa.leolini@unifi.it (L. Leolini).

https://doi.org/10.1016/j.eja.2018.06.006
Received 2 December 2017; Received in revised form 24 April 2018; Accepted 8 June 2018
Available online 21 July 2018
1161-0301/ © 2018 Elsevier B.V. All rights reserved.

yield and quality that may locally reduce or emphasize the impact of a warmer climate. As an example, the earlier occurrence of budbreak date in some cases increased the frequency of frost events in early spring leading to shoot damages and yield losses (Mullins et al., 1992; Narciso et al., 1992) as documented in outstanding wine regions as the French Champagne (Brun and Cellier, 1992) and the Luxembourgish (Molitor et al., 2014). Further, the combination of a shorter cycle with the occurrence of heat stress during and after fruit set phase has been associated with a decrease of berries growth, leading to the end of sugar accumulation (Greer and Weston, 2010), up to their abscission (Kliewer, 1977).

Despite the recognized limitations of current process-based crop models (Asseng et al., 2013; Moriondo et al., 2015; Rötter et al., 2011), they are considered as the only viable mean to obtain reliable projections of crop yield in response to climate variability (Bannayan and Crout, 1999), as they can deal with the non-linear interactions between environmental drivers and plant physiology, also considering the use of management practices to reduce the effect of climate change (Donatelli et al., 2006; Fraga et al., 2016; Therond et al., 2011).

Here we present a software library, UNIFI.GrapeML, implementing a set of modelling approaches for the simulation of the main physiological processes related to grapevine growth and development. We used the BioMA software architecture (www.biomamodelling.org), which adopts the component-oriented programming to develop software units which can be shared among the modelers community and extensible with new/alternative approaches (Donatelli et al., 2010, for application examples see Bregaglio and Donatelli, 2015; Cappelli et al., 2014; Donatelli et al., 2014; Stella et al., 2014). We then developed a new grapevine simulator using UNIFI.GrapeML, and we coupled it with a soil water model to release a modelling solution reproducing vine growth and development as affected by water stress. Accordingly, the main advantage of the UNIFI.GrapeML architecture is to allow easier implementations and maintenance of the modelling approaches which can be useful for investigating the emerging issues of agriculture in a context of climate change (e.g. extreme events around flowering, phenology dormancy period, water stress effect on biomass partitioning, etc.). We finally demonstrated the capability of this BioMA modelling solution to be interfaced with platform specific sensitivity analysis and automatic optimization tools, using an experimental dataset collected on a Spanish grapevine orchard (1998–2012, Chardonnay variety) as a case study.

2. Materials and methods

Fig. 1 presents the activities performed in this study, with a reference to the BioMA tools used for code generation and model analysis. After the development of the UNIFI.GrapeML software library (*Step A*, Sections 2.1 and 2.2), we developed a new model using available approaches for the reproduction of grapevine morpho-physiological processes at different plant ages. We then coupled it with a set of models to simulate crop water uptake and soil water redistribution in the soil profile (*Step B*, Section 2.3.1). The parameters of this modelling solution were calibrated to reproduce observed phenological development in an experimental vine orchard in 1998–2012 (*Step C*, Section 2.3.2). This activity laid the basis for a two-step global sensitivity analysis: at first, a screening method (i.e., Latin Hypercube Sampling) was applied on all the parameters of the modelling solution (*Step D*, Section 2.3.3); then the sub-set of the most important parameters was further inspected using a variance-based method (Sobol' Total Variance, *Step E*, Section 2.3.3). Using the information coming from the sensitivity analysis, an automatic calibration allowed to increase the accuracy of the modelling solution in reproducing the reference soil water content and yield data (*Step F*, Section 2.3.4).

2.1. Component architecture

UNIFI.GrapeML is a BioMA component collecting models of the main physiological processes of grapevine. The definition of the input/output (I/O) data structures (UNIFI.GrapeML.Interfaces) is separated from the modelling approaches which use them (UNIFI.GrapeML.Strategies), according to an implementation of the Bridge pattern (Fig. 2; Del Furia et al., 1995), in order to let third parties to extend and re-use the modelling domain in custom applications.

I/O variables are collected in domain classes, according to the ontology proposed by Forrester (1961) for System Dynamics. The domain classes of UNIFI.GrapeML are States (states variables, e.g., leaf area index, grape aboveground biomass), Rates (rates variables, e.g., rate of change of leaf area index), Auxiliary (intermediate derived variables, e.g., budbreak date), Exogenous (driving variables, e.g., maximum and minimum air temperature) and ExternalStates (state variables simulated by other components, e.g., soil water content). The CRA.ModelLayer.Core component, from which UNIFI.GrapeML depends, provides methods to perform the quality check of input (pre-conditions) and output (post-conditions) variables and model parameters, according to their ontology (minimum, maximum and default value, unit, type, and description).

Models are implemented in UNIFI.GrapeML.Strategies as *simple strategies* (e.g. ShootLeafNumber and LeafAreaGrowth; Fig. 3), which are units of code (C# classes) isolating an algorithm for a specific morpho-physiological process of grapevine. *Composite strategies* (e.g., LeafAreaIndex; Fig. 3) allow to compose *simple strategies* into higher-level models to represent part-whole hierarchies, while keeping the same programming interface. Available composite strategies refer to plant macro-processes as phenological development, evapotranspiration, leaf growth and biomass accumulation, biomass partitioning, extreme events affecting fruit biomass.

Context strategies (Strategy design pattern, e.g., Phenology; Fig. 3) are used to switch between *simple* or *composite strategies* presenting alternative modelling approaches for the same process (e.g., chilling-forcing (CF) unit or growing degree days (GDD) to simulate vine development) or to user choices (e.g., activation of extreme events in limiting fruit set).

2.2. Model description

The workflow of the *strategies* currently implemented in UNIFI.GrapeML is showed in Fig. 3. Phenological development starts with the accumulation of chilling units from a user-defined day of the year and continues until the end of the endo-dormancy period. Afterwards, forcing units are accumulated until budbreak (Section 2.2.1). Then, leaf appearance and expansion on shoots are simulated to derive the total plant leaf area and the leaf area index (Section 2.2.2). The emission of leaf area index triggers the light interception, which is converted into biomass, using a radiation use efficiency (RUE) approach. The daily value of RUE is modulated according to CO_2 concentrations and as a function of air temperature (Ritchie and Otter, 1984; Van Keulen and Seligman, 1987; Section 2.2.3). The daily growth rate of aboveground biomass is entirely allocated into vegetative organs from budbreak to flowering, whereas it is partitioned to fruits during flowering-harvest period according to user-defined coefficients. The fruit biomass is thus reduced according to the fruit set index based on the effect of high or low temperatures around flowering (Sections 2.2.4 and 2.2.5). A water stress index (Fractional Transpirable Soil Water, FTSW, 0–1), computed as the ratio between the Available Transpirable Soil Water in the rooted zone (ATSW) and the Total Transpirable Soil Water (TTSW) acts reducing the leaf development and transpiration (Bindi et al., 2005; Section 2.2.6) and stimulating root elongation (Bota et al., 2004; Dry et al., 2000). The minimum dataset of input meteorological data to run the model includes daily data of maximum and

	Activity	Objective	BioMA tools
Step A	Development of the UNIFI.GrapeML software component	Release of a software library with models for vine development and growth	Domain Class Coder (DCC) API Class Coder (ACC) Strategy Class Coder (SCC)
Step B	Coupling UNIFI.GrapeML with models for soil water uptake and redistribution	Release of a new grapevine model to reproduce the impact of soil water availability on vine growth and yield	Composition Layer Interactive Coder (CLIC)
Step C	Calibration of the phenological development using field observations (multi-start simplex method)	Adjustment of the simulation of the main phenological stages before running the sensitivity analysis	Optimizer, automatic calibration tool
Step D	Sensitivity analysis with the Latin Hypercube Sampling method	Screening of the most relevant parameters in influencing simulated fruit biomass variability	Library User Interface for Sensitivity Analysis (LUISA)
Step E	Sensitivity analysis with the Sobol' Total Variance method	Identification of the subset of parameters to be automatically calibrated	Library User Interface for Sensitivity Analysis (LUISA)
Step F	Calibration of the fruit biomass accumulation using field observations (multi-start simplex method)	Demonstrate the capability of the modelling solution to simulate the year-to-year yield variability	Optimizer, automatic calibration tool

Fig. 1. Workflow of the activities presented in this study, with relevant objectives and BioMA tools, downloadable at www.biomamodelling.org.

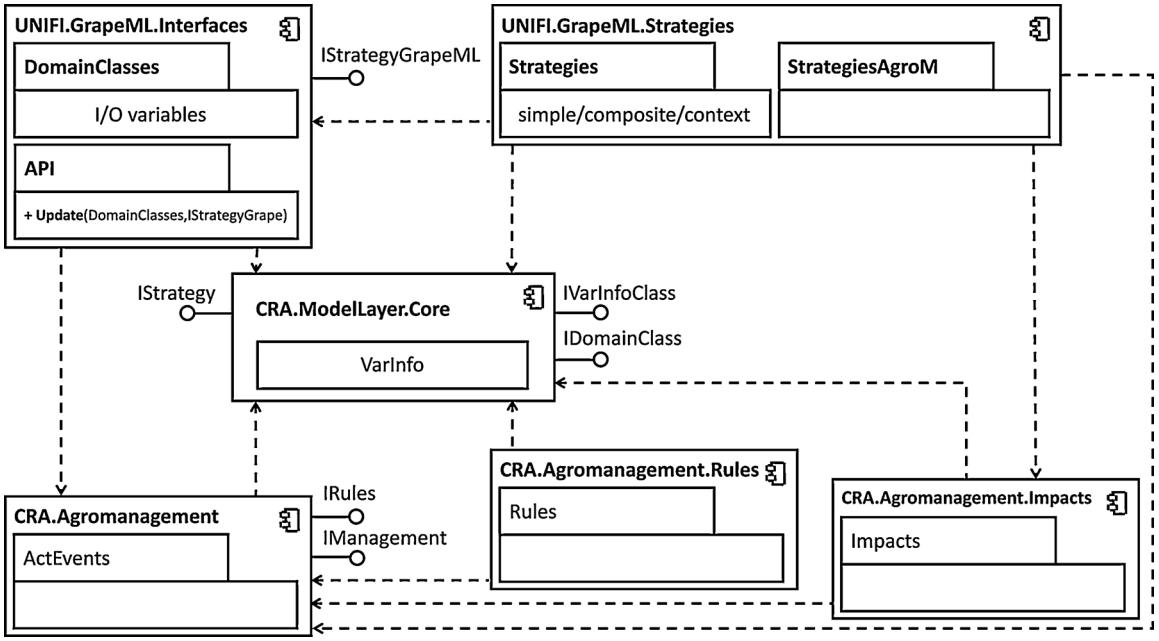

Fig. 2. Unified Modelling Language (UML) component diagram of the UNIFI.GrapeML component. Software units (UNIFI.GrapeML.Interfaces and UNIFI.GrapeML.Strategies) have a dependency (arrow dashed line) to CRA.ModelLayer.Core and CRA.Agromanagement component, belonging to the core of the BioMA framework.

minimum air temperature, global solar radiation and precipitation, other than the CO_2 atmospheric concentration.

2.2.1. Phenological development

2.2.1.1. Chilling-forcing method. A parallel CF approach (Caffarra and Eccel, 2010) is available in UNIFI.GrapeML. The dormancy period until budbreak date is simulated considering the accumulation of chilling and forcing units. The chilling units accumulation starts at the end of the previous growing season and ends when a chilling requirement threshold is reached, then the accumulation of thermal units (forcing units) begins. The effect of chilling accumulation on forcing units decreases from the first day of chilling accumulation up to the day when the effect of chilling temperature on forcing units ends (Table 1; Eqs. (1)–(3)). Budbreak is reached when both chilling and forcing requirements are satisfied. The subsequent estimation of flowering, veraison, and maturity dates is performed using three sigmoid curves of forcing accumulation and defined by three thresholds of forcing requirement (Table 1; Eqs. (4)–(6)).

2.2.1.2. Growing degree days approach. UNIFI.GrapeML provides an alternative model for phenological development, based on the accumulation of growing degree days (GDD, °C d^{-1}, Bindi et al., 1997a). GDD are accumulated starting from a user-defined day of the year until the fulfillment of the thermal requirementfor budbreak (Eq.

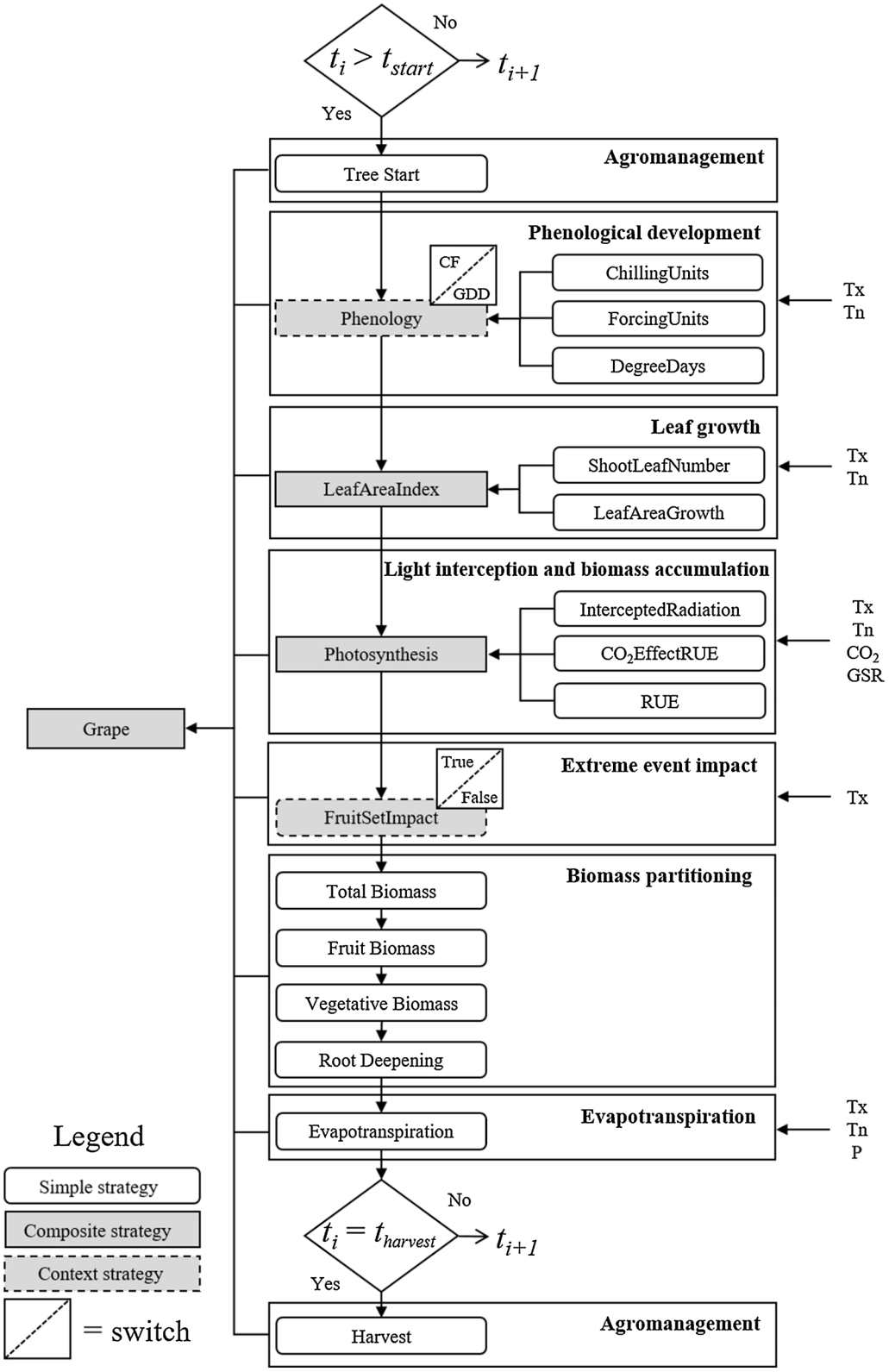

Fig. 3. Workflow of the strategies currently implemented in UNIFI.GrapeML. The scheme presents the logical order in which models are called during a daily time step. T_x = daily maximum air temperature (°C), T_n = daily minimum air temperature (°C), P = precipitation (mm d^{-1}), GSR = global solar radiation (MJ m^{-2} d^{-1}), CF = Chilling-Forcing, GDD = Growing Degree Days (°C d^{-1}).

(7)).

$$GDD = \sum_{t_0}^{t_1} T_{avg} - BaseTemperature \quad (7)$$

where T_{avg} is the daily average air temperature (°C), t_0 is the starting day for GDD accumulation, t_1 is the day when phenological phase is reached (budbreak, flowering, veraison, and maturity) and *BaseTemperature* (°C) is the base temperature for GDD accumulation. GDD are accumulated only if T_{avg} is higher than *BaseTemperature*

Table 1
Equations of the chilling-forcing method to simulate phenological development in the four main phenological stages of grapevine (Caffarra and Eccel, 2010).

Phenological phases	Equations	
Budbreak	$ChillingUnit = \sum \frac{2}{1+e^{aParam(T_{avg}-cParam)^2}}$	(1)
	$Forcing\ Budbreak = \sum \frac{1}{1+e^{db(T_{avg}-eb)}}$	(2)
	$ForcingCritic = Col \cdot e^{co2 \cdot ChillingUnit}$	(3)
Flowering	$Forcing\ Flowering = \sum \frac{1}{1+e^{df(T_{avg}-ef)}}$	(4)
Veraison	$Forcing\ Veraison = \sum \frac{1}{1+e^{dv(T_{avg}-ev)}}$	(5)
Maturity	$Forcing\ Maturity = \sum \frac{1}{1+e^{dm(T_{avg}-em)}}$	(6)

ForcingCritic = critical number of forcing units required to reach budbreak; *aParam*, *Col*, *co2* = curve shape parameters; *cParam* = optimal chilling temperature; T_{avg} = daily average air temperature; *db*, *df*, *dv*, *dm* = forcing units rates and *eb*, *ef*, *ev*, *em* = inflection points of the sigmoid functions.

otherwise GDD accumulation rate is equal to zero. Then, GDD are computed until flowering, when a minimum number of leaves (model parameter) is used to trigger flowering stage. GDD accumulation is also computed for the lag phase when berry weight does not increase; then, the veraison stage is triggered and GDD are accumulated until the maturity stage.

2.2.2. Leaf growth

Leaf area growth is simulated as a function of leaf appearance and expansion on the actively growing shoots adjusted for water stress (Bindi et al., 1997a, b; Eqs. (8)–(10)).

$$LeafAppearanceStress = 1/(1 + SLN1 \cdot e^{-SLN2 \cdot FTSW}) \quad (8)$$

$$LeafNumberRate = (SLNI + LAR1 \cdot T_{avg}) \cdot (1 + LAR2 \cdot ShootLeafNumber) \cdot LeafAppearanceStress \quad (9)$$

$$ShootLeafNumberStress = ShootLeafNumberStress + LeafNumberRate \quad (10)$$

where *LeafNumberRate* is the daily rate of leaf appearance (number of leaves d^{-1}), *SLNI* (Shoot Leaf Number Intercept, number of leaves d^{-1}), *LAR1* (Leaf Appearance Rate 1, number of leaves $d^{-1}\,°C^{-1}$) and *LAR2* (Leaf Appearance Rate 2, number of leaves^{-1}) are curve shape parameters, *SLN1* (unitless) and *SLN2* (unitless) are the parameters of water stress impact on *LeafNumberRate*. FTSW (unitless) is a water stress index which impacts on the number of leaves appeared on the shoot and, consequently affect leaf development (*ShootLeafNumberStress*, number of leaves; Bindi et al., 2005). The total leaf area per shoot (*ShootLeafArea*, cm^2; Eq. (11)) and plant leaf area (*PlantLeafArea*, cm^2; Eq. (12)) are finally computed during season progress considering the number of shoot per plant:

$$ShootLeafArea = SLAS \cdot (ShootLeafNumberStress)^{SLAE} \quad (11)$$

$$PlantLeafArea = ShootLeafArea \cdot ShootNumber \quad (12)$$

where *SLAS* (Shoot Leaf Area Slope, cm^2 number of leaves^{-1}) and *SLAE* (Shoot Leaf Area Exponential, unitless) are curve shape parameters and *ShootNumber* is the number of shoots per plant. Finally, *LeafAreaIndex* ($m^2\,m^{-2}$; Eq. (13)) is computed considering the soil occupied by the plant (*PlantArea*, m^2) and the proportion of the area shaded by plant (*ProportionShadedArea*, unitless).

$$LeafAreaIndex = (PlantLeafArea/10000)/(ProportionShadedArea \cdot PlantArea) \quad (13)$$

2.2.3. Light interception and biomass accumulation

Biomass accumulation is simulated considering the radiation intercepted by the canopy and the radiation use efficiency (RUE, g MJ^{-1}) affected by air temperature and CO_2 concentration.

The fraction of radiation intercepted (*RadIntercepted*, unitless; Eq. (14)) is calculated using the Beer-Lambert law (Monsi and Saeki, 1953), considering the *LeafAreaIndex* ($m^2\,m^{-2}$) and the crop extinction coefficient (*CropCoeff*, unitless).

$$RadIntercepted = 1 - e^{(-CropCoeff \cdot LeafAreaIndex)} \quad (14)$$

RUE (g MJ^{-1}; Eq. (15)) represents the effective biomass accumulated per unit of global solar radiation, modulated by the effect of temperature. It is calculated multiplying a maximum RUE initial value CO_2-dependent (*RUEmax*) by a temperature function (Eq. (15); Bindi et al., 2001a, b).

$$RUE = RUEmax \cdot (1 - 0.0025 \cdot (0.25 \cdot T_n + 0.75 \cdot T_x - 25)^2) \quad (15)$$

where *RUEmax* assumes different values depending on CO_2 atmospheric concentration (CO_2; Eq. (16)–(18)), T_x is the daily maximum air temperature, and T_n is the daily minimum air temperature. Accordingly, if CO_2 is equal to 350 ppm:

$$RUEmax = InitialRUE \quad (16)$$

where *InitialRUE* is equal to 1.001 g MJ^{-1}. If $CO_2 > 350$ ppm and $CO_2 \leq 550$ ppm:

$$RUEmax = mRUE550 \cdot CO_2 + qRUE550 \quad (17)$$

While if $CO_2 > 550$ ppm and $CO_2 \leq 700$ ppm:

$$RUEmax = mRUE700 \cdot CO_2 + qRUE700 \quad (18)$$

where CO_2 is the atmosphere CO_2 concentration (ppm), *mRUE550* (g $MJ^{-1}\,ppm^{-1}$), *qRUE550* (g $MJ^{-1}\,ppm^{-1}$), *mRUE700* (g $MJ^{-1}\,ppm^{-1}$), and *qRUE700* (g $MJ^{-1}\,ppm^{-1}$) are empirical parameters for the linear increase of *RUEmax* (g MJ^{-1}) according to different CO_2 concentration thresholds. Finally, the daily photosynthesis rate of the plant (*PhotoRate*, g $m^{-2}\,d^{-1}$; Eq. (20)) is calculated taking into account *GSR*, *RadIntercepted*, *ProportionShadedArea*, and the water stress effect (unitless) on the daily photosynthesis rate (*PhotoStress*, g $m^{-2}\,d^{-1}$; Eq. (19)).

$$PhotoStress = 1/(1 + PHO1 \cdot e^{-PHO2 \cdot FTSW}) \quad (19)$$

$$PhotoRate = GSR \cdot RadIntercepted \cdot ProportionShadedArea \cdot RUEmax \cdot PhotoStress \quad (20)$$

2.2.4. Extreme event impact

The impact of extreme events on fruit set is simulated according to a fruit set index (*FruitSetIndex*, unitless; Eq. (21)), considering the impact of the 7-days average maximum air temperatures around flowering stage.

FruitSetIndex (ranging from 0 to 1) is modulated as the temperature factor function such as described after Farquhar and Caemmerer (1982) for photosynthesis (Eq. (21)):

$$FruitSetIndex = \left(\frac{T - T_{min}}{T_{opt} - T_{min}}\right)^q \cdot \left(\frac{T_{max} - T}{T_{max} - T_{opt}}\right) \quad (21)$$

where T is the 7-days average maximum air temperature (°C), T_{max}, T_{opt} and T_{min} (°C) are the maximum, optimum and minimum air temperature for optimal fruit set, and q (unitless) is a curve shape parameter.

2.2.5. Biomass partitioning

The current cumulated aboveground biomass (*TotBio*, g m^{-2}; Eq. (22)) is computed as sum of the daily photosynthesis rates (Eq. (20)):

$$TotBio = TotBio + PhotoRate \quad (22)$$

The partitioning of the epigeal biomass between vegetative and fruit biomass is driven by phenological phases. Before flowering (*TriggerBudbreak* = 1 and *TriggerFlowering* = 0), the daily rate of aboveground biomass is entirely allocated to the vegetative pool

(*VegBio*, g m^{-2}; Eqs. (23) and (25)) while after blooming fruit biomass (*FruBio*, g m^{-2}; Eq. (24)) is computed using a linear relationship between the aboveground biomass and a daily-increasing harvest index ($\sum HI$) calculated after anthesis as the sum of daily fractions (*HI,* d^{-1}) of the maximum final attainable harvest index. The *FruBio* is affected by the value of *FruitSetIndex* estimated after flowering.If *TriggerBudbreak* > 0 and *TriggerFlowering* < 1:

$$VegBio = TotBio \tag{23}$$

If *TriggerFlowering* > 0:

$$FruBio = TotBio \cdot \sum HI \cdot FruitSetIndex \tag{24}$$

$$VegBio = TotBio - FruBio \tag{25}$$

Finally, the biomass partitioned to the root system is computed in terms of root deepening into the soil. According to Nendel and Kersebaum (2004), a vineyard shows a very low root growth rate when it reaches maturity stage. Furthermore, Dry et al. (2000) demonstrated that low water availability stimulates root growth increase. In UNIFI.GrapeML, the root elongation (*RootDepthRate*, cm d^{-1}; Eqs. (26) and (27)) in wet conditions is driven by a basic growth rate (*RootGrowthBasic*, cm d^{-1}), while in water stress conditions (*FTSWLimitRoot* = 0.5 and *DayForStress* = 2) is computed as a function of a water-stressed growth rate (*RootGrowthStress*, cm d^{-1}):If *FTSW* > *FTSWLimitRoot*:

$$RootDepthRate = RootGrowthBasic \tag{26}$$

If *FTSW* < *FTSWLimitRoot* and *DayCountStress* > *DayForStress*:

$$RootDepthRate = RootGrowthStress*(1 - FTSW) \tag{27}$$

2.2.6. Evapotranspiration

The crop transpiration rate is estimated considering the *PhotoRate* (g m^{-2} d^{-1}), the air vapor pressure deficit (*VPD*, kPa), and the transpiration efficiency coefficient (*TEC*, Pa; Tanner and Sinclair, 1983) representing the accumulated biomass per gram of water transpired by the plant (Eq. (28)):

$$TranspirationRate = \frac{PhotoRate \cdot VPD}{TEC} \tag{28}$$

The *TranspirationRate* of the previous equation expressed in mm d^{-1} then is converted in cm d^{-1}.

Moreover, the crop potential evaporation rate (mm d^{-1}) is calculated considering the radiation intercepted by the plant, as described in (Soltani and Sinclair, 2012; Eqs. (28) and (29)).

$$Delta = e^{\left(21.255 - \frac{5304}{273 + T_{avg}}\right) \cdot \frac{5304}{(273 + T_{avg})^2}} \tag{29}$$

$$EvaporationRate = \frac{0.25 \cdot GSR + 0.75 \cdot GSR \cdot RadIntercepted \cdot Delta + 0.68 \cdot 0.4 \cdot VPD}{Delta + 0.68} \tag{30}$$

where T_{avg} is the daily average air temperature, *GSR* is the global solar radiation, *RadIntercepted* the intercepted radiation and *Delta* (mbar K^{-1}) is the slope of the saturated vapor pressure deficit curve.

Then, potential evaporation is, in turn, converted into actual evaporation decreasing its value as a function of the elapsed days (*LastDayRain*) from the last rainfall event (Amir and Sinclair, 1991; Soltani and Sinclair, 2012). Then, the actual daily evapotranspiration is accounted considering the evaporation and transpiration rate (Eq. (31)):

$$EvapotranspirationRate = EvaporationRate + TranspirationRate \tag{31}$$

The UNIFI.GrapeML does not still include any model to compute soil water availability and dynamics and the associated root water uptake, which are needed as input (ExternalRates domain class) to compute water stress. The impact of water stress is thus activated when the component is coupled to a soil model, as demonstrated in the case study presented below.

2.3. Case study

2.3.1. Modelling solution development

The strategies implemented in UNIFI.GrapeML were composed to give a new grapevine model simulating the whole processes connected to growth and development, represented by the *composite strategy* Grape in Fig. 3. The model was then coupled with the two components: UNIMI.SoilW (Donatelli et al., 2014), collecting models to simulate crop water uptake and redistribution in the soil profile, and CRA.AgroManagement (Donatelli et al., 2006), which handles the implementation of agricultural management events. The resulting modelling solution (MS; Fig. A.1 in Supplementary Material) was developed with the software CLIC (Composition Layer Interactive Coder, www.biomamodelling.org).

The soil profile was split into nine layers (1^{st}-2^{nd} layer = 0.05 m, 3^{rd}-9^{th} layer = 0.2 m) and soil water redistribution was simulated with a tipping-bucket approach (Ritchie, 1998), assuming that water can move to the *(i+1)-th* layer when field capacity of the *i-th* layer is exceeded. The root depth simulated by UNIFI.GrapeML is used as input to compute crop water uptake, which considers crop potential transpiration as the plant demand, according to the EPIC model (Williams et al., 1989). Soil evaporation was derived by daily evapotranspiration considering the fraction of light intercepted by the canopy (Ritchie, 1974), setting an evaporation layer of 0.1 m. The minimum and maximum soil water content in each layer were set to wilting point and field capacity, respectively, both derived by pedo-transfer functions from soil texture. The interception of precipitation by the canopy was computed according to Von Hoyningen-Huene (1981), with the remaining quote infiltrating into the soil.

CRA.AgroManagement is a software component to simulate the timing and the effects of management events in an agricultural simulation model (Donatelli et al., 2006). It formalizes the decision making process via the rule-impact approach: a management action requires that a set of conditions based on the state of the system (a "rule") is met to be applied. When it happens, a management action is triggered. This approach allows de-coupling the agro-management operations from biophysical models. In this study, we used it to set the starting day of year (244) for chilling units accumulation and the end of the grape growing season (305), respectively.

2.3.2. Experimental reference dataset

We selected a vineyard located about 40 km Northwest (NW) of Barcelona in the Catalan Prelitoral Depression (lat. 41.53 °N, long. 1.77 °E, 340 m. a.s.l., Penedès Depression) as the location of our case study. This area has a long tradition of vine cultivation within the Designation of Origen Penedès, with vines representing about 80% of the cultivated land (IDESCAT, 2013). The climate is Mediterranean, with average maximum (T_x) and minimum (T_n) air temperatures in 1998–2012 during budbreak-flowering equal to 19.7 °C (standard deviation, SD = 1.3 °C) and 8.9 °C (SD = 0.8 °C), respectively, whereas during veraison-harvest period equal to 30.3 °C (T_x, SD = 1.7 °C) and 18.7 °C (T_n, SD = 1.7 °C). Precipitation are mainly concentrated in spring, with average cumulated values of 118.8 ± 71.2 mm, and then decrease during veraison-harvest phase (cumulated values = 39.9 ± 17.7 mm; Table 2). The soil of the experimental vineyard is Typic Xerorthents and Fluventic Haploxerepts (Soil map of the Penedès, DAR, 2008), with soil depth ranging from 0.8 to 1.5 m. Soil particle distribution (Gee and Bauder, 1986) and organic matter content (Allison, 1965) were evaluated in samples collected at three locations (up, mid and down slope). The soil texture is loam, with bulk density equal to 1.5 g cm^{-3}, and organic matter = 1.3% (Ramos and Martínez-Casasnovas, 2014).

Trained vines of Chardonnay variety (3.1 m × 1.3 m, 16 nodes per

Table 2
Average and standard deviation of maximum and minimum air temperatures, cumulated precipitation and reference evapotranspiration in the grape growing seasons (1998–2012) in the study area.

Meteorological variables	Units	Budbreak-Flowering	Flowering-Veraison	Veraison-Maturity
Maximum temperature	°C	19.7 ± 1.3	27.6 ± 1.4	30.3 ± 1.7
Minimum temperature	°C	8.9 ± 0.8	15.8 ± 0.9	18.7 ± 1.03
Precipitation	mm	118.8 ± 71.2	65.8 ± 51.1	39.9 ± 17.7
Evapotranspiration	mm	296.5 ± 47.4	413.6 ± 76.3	241.9 ± 56.7

vine) were planted after land levelling in 1989. The vineyard is orientated NNE-WSW, with 7% average slope. Phenological observations in 1998–2012 were available at budbreak (BBCH code 7), flowering (BBCH code 65), veraison (BBCH code 81) and harvest. No evaluation of Brix percentage was carried out in the experimental trials, therefore we assumed as maturity date the harvest date to calibrate the vine phenological development. Grape fresh yield (t ha^{-1}) in 1998–2010 was provided by the farmer owner of the orchard, whereas in 2011–2012 the yield was collected on 15 plants (Ramos and Martínez-Casasnovas, 2014). Dry fruit biomass was derived as the 23% of total berry fresh weight as showed by some authors for specific conditions (Garcia de Cortazar-Atauri et al., 2009b; Girona et al., 2009). Soil water content was measured in two cropping seasons (2011–2012) at four soil depths (0.3 m; 0.5 m; 0.7 m; 1 m), using soil moisture probes (Time Domain Reflectometry, TDR). Daily meteorological data as input for the models were obtained from a weather station placed in close proximity to the orchard (Els Hostalest de Pierola, 41.53 °N; 1.81 °E; 316 m a.s.l.). Available variables were maximum and minimum temperature, precipitation and wind speed in the period 1997–2012 (Tables 2 and A.2 in Supplementary Material). Global solar radiation was estimated using the Hargreaves method (Hargreaves and Samani, 1982), reference evapotranspiration via Penman-Monteith equation (Monteith, 1965).

2.3.3. Sensitivity analysis experiment

The modelling solution presented in Section 2.3.1. was interfaced with a library of methods for model sensitivity analysis, LUISA (Library User Interface for Sensitivity Analysis, Donatelli et al., 2009, available at www.biomamodelling.org), to evaluate the contribution of model parameters and of their interaction on the variability of simulated grape yield at harvest.

A two-step global sensitivity analysis was performed (Confalonieri et al., 2010; Saltelli et al., 1995, 1999). A screening regression method (Latin Hypercube Sampling, LHS; McKay et al., 1979) was used to select the most relevant parameters of the modelling solution at a low computational expense (Table 3). In the second step, the subset of parameters explaining most output variability was evaluated with the Sobol' variance-based method, to decompose it into fractions to be attributed to each parameter or sets of parameters.

The LHS regression method independently and randomly samples each parameter without replacement, to give a matrix of X rows (number of samplings) and n columns (number of varied parameters). The modelling solution was iteratively run using each combination of parameter values, and grape yield was recorded after each simulation. The non-parametric Spearman's correlation between each parameter under evaluation and the model output was then computed, as suggested for biophysical models by Bellocchi et al. (2010) and Zacharias et al. (1996). This screening method was applied for each cropping season in the period 1998–2012, in order to quantify the variation of model sensitivity to parameters change under varying weather conditions. The model parameters related to phenological development were excluded from the sensitivity analysis, as they were calibrated to match reference data (see Section 2.3.4). Model parameters were sampled from a uniform distribution ranging from -15% to +15% of default values (Table 3). The LHS method was run by setting the convergence to 0.025 (i.e., the maximum difference of average Spearman's correlation between model parameters and grape yield in two consecutive evaluations). The convergence was firstly evaluated after 6000 runs, and then every 1000 runs.

The parameters with average Spearman's correlation higher than 0.1 ± 0.025 in the 15 years were then investigated with the Sobol' method. This method, recognized as a standard in global sensitivity analysis applied to biophysical simulation models (Stella et al., 2014; Varella et al., 2010), highlights the portion of the total variance explained by the contribution of the single parameters, or even including parameter interactions (Tang et al., 2007). This second step of sensitivity analysis was performed with the same settings for model parameter values and for input weather data used by the LHS method. Convergence was expressed as the maximum difference of Sobol' Total Order index in two consecutive runs and set to 0.01, with a first check after 85,000 runs, and then testing it every 17,000 runs.

2.3.4. Calibration and evaluation of the modelling solution

The modelling solution was coupled with the Optimizer software application (available at www.biomamodelling.org), to perform automatic calibration of parameter values to increase its accuracy in reproducing reference data. The thermal requirements of the chilling-forcing approach to reach budbreak, flowering, veraison and maturity stage were calibrated prior to perform sensitivity analysis, by minimizing root mean square error between simulated and reference data, considering a calibration range within ± 60% around default values (Caffarra and Eccel, 2010; Table 3).

Dates of budbreak, flowering and veraison were recorded as field observations, whereas we assumed a correspondence between the maturity and the harvest date, as no measurements of Brix degree were available in experimental data.

The most relevant parameters from sensitivity analysis were subjected to automatic calibration using the multi-start downhill simplex algorithm (Nelder and Mead, 1965) as modified by Acutis and Confalonieri (2006). This algorithm explores the N-dimensional parameter space, with N as the number of the parameters under evaluation, following the gradient of the objective function, which in our case was the Root Mean Square Error (RMSE). A geometrical figure with N + 1 vertexes (i.e., the simplex) is created when the optimization starts, with N as the number of parameters under evaluation. After each simulation run, the objective function is evaluated at each vertex of the simplex, which moves via reflection, contraction, or expansion towards the minimization of RMSE between reference and simulated data. The optimization ends when the difference of RMSE value in the simplex vertexes is below a tolerance range (i.e., 0.001). We used five simplexes at each optimization run, with the same domain of model parameters used for the sensitivity analysis assessment.

The evaluation of model performance in reproducing phenology, soil water content and fruit dry biomass was based on the following statistical metrics (Green and Stephenson, 1986; James and Burges, 1982; Loague and Green, 1991; Eqs. (32)–(36)):Root Mean Square Error (RMSE, Eq. (32)):

$$RMSE = \left[\sum_{i=1}^{n} \frac{(P_i - O_i)^2}{n}\right]^{0.5} \quad (32)$$

and the normalized form (RRMSE, Eq. (33)):

$$RRMSE = RMSE \cdot \frac{100}{\overline{O}} \quad (33)$$

Coefficient of Residual Mass (CRM, Eq. (34)):

$$CRM = \frac{(\sum_{i=1}^{n} O_i - \sum_{i=1}^{n} P_i)}{\sum_{i=1}^{n} O_i} \quad (34)$$

Table 3
Acronyms, description, default value and unit of the model parameters evaluated via sensitivity analysis, with relevant source of information. CU = Chilling Units, FU = Forcing Units.

Parameter	Description	Min	Max	Default	Unit
Phenological development					
aParam	Curve shape parameter	0.002	0.008	0.005[a]	unitless
cParam	Optimal chilling temperature	1.12	4.48	2.8[a,b,c,d,e]	°C
ChillingReq	Chilling requirement	31.48	125.91	78.692[a]	CU
db	Slope of forcing unit equation for budbreak	−0.42	−0.11	−0.26[a]	unitless
df	Slope of forcing unit equation for flowering	−0.42	−0.11	−0.26[a]	unitless
dv	Slope of forcing unit equation for veraison	−0.42	−0.11	−0.26[a]	unitless
dm	Slope of forcing unit equation for maturity	−0.42	−0.11	−0.26[a]	unitless
eb	Inflection point for budbreak	6.41	25.70	16.06[a]	°C
ef	Inflection point for flowering	6.41	25.70	16.06[a]	°C
ev	Inflection point for veraison	6.41	25.70	16.06[a]	°C
em	Inflection point for maturity	6.41	25.70	16.06[a]	°C
Col	Curve shape parameter	70.50	282.02	176.26[a]	unitless
co2	Curve shape parameter	−0.024	−0.006	−0.015[a]	unitless
LimitForcingReq	Last day of chilling effect on forcing requirement	94	374	234[a]	d
FloweringReq	Forcing requirement for flowering	9.88	39.54	24.71[a,b,d,e]	FU
VeraisonReq	Forcing requirement for veraison	20.46	81.82	51.146[a,b,d,e]	FU
MaturityReq	Forcing requirement for maturity	–	–	–	FU
Leaf growth					
ShootNumber	Number of shoots per plant	13.6	18.4	16[i]	n° of shoots
SLNI	Curve shape parameter of Shoot Leaf Number equation	−0.32	−0.24	−0.28[f]	n° of leaves d^{-1}
LAR1	Curve shape parameter of Shoot Leaf Number equation	0.03	0.05	0.04[f]	n° of leaves d^{-1} $°C^{-1}$
LAR2	Curve shape parameter of Shoot Leaf Number equation	−0.017	−0.013	−0.015[f]	n° of leaves^{-1}
SLAS	Curve shape parameter of Shoot Leaf Area equation	4.58	6.2	5.39[f,h]	cm^2 n° of leaves^{-1}
SLAE	Curve shape parameter of Shoot Leaf Area equation	1.81	2.45	2.13[f]	unitless
ProportionShadedArea	Proportion of the area shaded by plant	0.64	0.86	0.75[f]	unitless
PlantingDensity	Squared meters of soil per plant	3.4	4.6	4[i]	m^2 plant^{-1}
SLN1	Coefficient of water stress equation on leaf development	22.09	29.80	25.9[j,k]	unitless
SLN2	Coefficient of water stress equation on leaf development	14.71	19.90	17.3[j,k]	unitless
Light interception and biomass accumulation					
CropCoeff	Extinction coefficient for intercepted radiation	0.51	0.69	0.6[l]	unitless
RUEmax	Initial RUE at CO_2 concentration of 350 ppm	0.85	1.15	1.001[f]	g MJ^{-1}
qRUE550	Intercept of the linear equation for CO_2 550 ppm	0.54	0.73	0.633[m]	g MJ^{-1}
mRUE550	Coeff. of the linear equation for CO_2 550 ppm	0.00089	0.0012	0.00105[m]	g MJ^{-1} ppm^{-1}
PHO1	Coefficient for water stress effect on photosynthesis	10.97	14.84	12.9[j,k]	unitless
PHO2	Coefficient for water stress effect on photosynthesis	11.99	16.22	14.1[j,k]	unitless
qRUE700	Intercept of the linear equation for CO_2 700 ppm	0.81	1.09	0.954[m]	g MJ^{-1}
mRUE700	Coeff. of the linear equation for CO_2 700 ppm	0.0004	0.00053	0.000468[m]	g MJ^{-1} ppm^{-1}
Biomass partitioning					
HI	Slope of Fruit Biomass Index equation	0.0038	0.0051	0.00443[f,h]	d^{-1}
HICutOff	Harvest Index cut off	0.43	0.58	0.5	d^{-1}
$Root_{ini}$	Initial value of root depth	85	115	100[n,i]	cm
RootGrowthBasic	Root growth rate for not limited water conditions	0.0009	0.0012	0.001	cm d^{-1}
RootGrowthStress	Root growth rate for limited water conditions	0.043	0.058	0.05	cm d^{-1}
FTSWLimitRoot	FTSW Limit for Root Growth	0.42	0.58	0.5	unitless
DayForStress	N° days after which water stress effect on root occurs	1.7	2.3	2	d
Evapotranspiration					
TEC	Transpiration efficiency coefficient	3.05	9.15	6.1[f,j]	Pa
Extreme event impact					
Tmax	Maximum temperature for fruit set at flowering	35	47	41[o,p,q,r]	°C
Tmin	Minimum temperature for fruit set at flowering	0.9	1.2	1[o,p,q,r]	°C
Topt	Optimum temperature for fruit set at flowering	21	28	25[o,p,q,r]	°C
q	Curve shape parameter	1.62	2.19	1.9[o,p,q,r]	unitless

References: [a]Caffarra and Eccel (2010); [b]Pouget (1963); [c]Pouget (1968); [d]Dokoozlian (1999); [e]Botelho et al. (2007); [f]Bindi et al. (1997a); [g]Dos Santos et al. (2003); [h]Bindi et al. (1997b); [i]Ramos and Martinez-Casasnovas (2014); [j]Bindi et al. (2005); [k]Lebon et al. (2006); [l]Poni et al. (2006); Palmer (1977); [m]Bindi et al. (2001a, 2001b); [n]derived by Nendel and Kersebaum (2004) considering a vineyard from 3 to 18 years; [o]derived by Kliewer (1977); [p]Ewart and Kliewer (1977); [q]Tukey (1958); [r]Haeseler and Fleming (1967).

Modelling Efficiency (EF, Eq. (35)):

$$EF = \frac{(\sum_{i=1}^{n}(O_i - \overline{O})^2 - \sum_{i=1}^{n}(P_i - O_i)^2)}{\sum_{i=1}^{n}(O_i - \overline{O})^2} \quad (35)$$

Pearson's Coefficient (r, Eq. (36)):

$$r = \frac{\sum_{i=1}^{n}(O_i - \overline{O_i})\cdot(P_i - \overline{P_i})}{\sqrt{\sum_{i=1}^{n}(O_i - \overline{O_i})^2 \cdot \sum_{i=1}^{n}(P_i - \overline{P_i})^2}} \quad (36)$$

where P_i are the predicted values, O_i are the observed values; n is the number of samples; and $\overline{O}$ is the mean of the observed data. The significance of the relationship between observed and predicted values was further tested with *F*-test.

3. Results and discussion

3.1. Sensitivity of modelling solution to weather variability and parameter changes

The results of the sensitivity analysis are presented in Fig. 4,

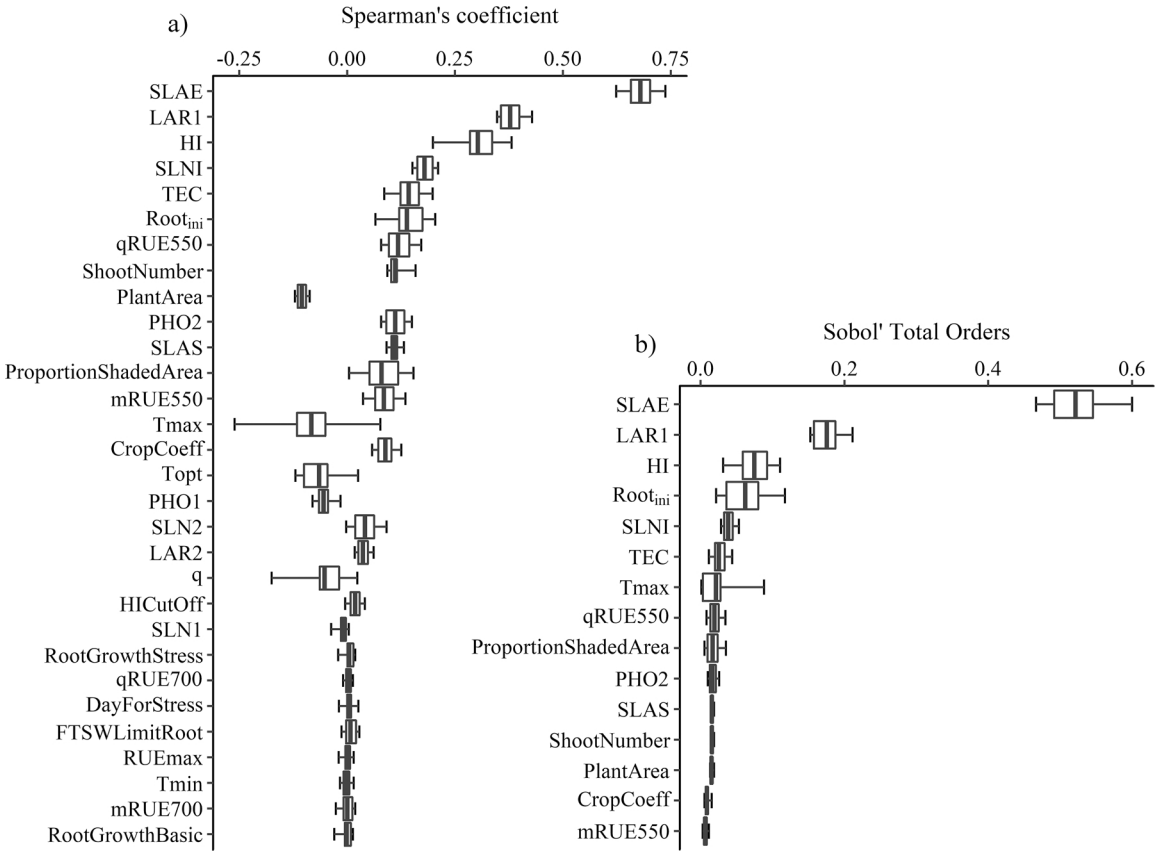

Fig. 4. Sensitivity Analysis using LHS and Sobol' methods. The Spearman's correlation coefficient (Fig. 4a) and Sobol' Total Order (Fig. 4b) were used as metrics to determine which parameters the modelling solution is more sensitive to.

showing the Spearman's correlation coefficient (*SC*; Fig. 4a) among model parameters and the fruit biomass variability, and Sobol' Total Orders (*STL*; Fig. 4b) computed on each parameter of the modelling solution.

According to LHS results, the two top ranked parameters in explaining the variability of fruit biomass were related to shoot leaf area growth, i.e., the exponential coefficient driving the shoot leaf area expansion (*SLAE*, Eq. (11)), and the slope of the temperature-dependent linear function related to the daily rate of leaf appearance (*LAR1,* Eq. (9)). The *SLAE* parameter showed a higher average Spearman's correlation ($\overline{SC}_{SLAE}$ = 0.680, coefficient of variation (cv.) 20%) than *LAR1* ($\overline{SC}_{LAR1}$ = 0.378, cv. 13%), suggesting that shoot leaf area expansion has a prominent influence on the simulated leaf area, which in turn resulted as the most relevant process in influencing fruit biomass. The key role of leaf area expansion is further proved by the high relevance of other connected empirical parameters, i.e., the intercept of the temperature-dependent linear function estimating shoot leaf number (*SLNI*, 4th ranked) and the slope of the shoot leaf area function (*SLAS*, 11th ranked). The third most important parameter in explaining fruit biomass variability was the harvest index (*HI*), which showed a high positive correlation with the model output ($\overline{SC}_{HI}$ = 0.3), with a large variability between years (cv. 17%): the higher the yield, the stronger the correlation. Our results agreed with Wang et al. (2013), who identified the parameters related to the leaf area expansion as the most relevant in affecting simulated corn yield variability in the WOFOST model, and with Ruget et al. (2002) and Dzotsi et al. (2013), who evidenced via sensitivity analysis that wheat, maize, peanut and cotton yields were mainly affected by leaf development and crop partitioning parameters. Another study by Wang et al. (2005) confirms that *HI* is one of the most sensitive parameters in crop models when yield is the target simulated variable and it is a part of a set of interactive parameters, using FAST sensitivity analysis on EPIC crop growth model.

The modelling solution (MS) showed a higher sensitivity to the parameters linked to the water use (transpiration efficiency coefficient, *TEC*, 5th ranked, and initial root length, *Root$_{ini}$*, 6th ranked) rather than to the ones modulating the radiation use efficiency (*mRUE550* and *qRUE550,* 7th ranked and 13th ranked, respectively). *Root$_{ini}$* determines the depth of the root zone, therefore it substantially impacted on the potential plant water reserve, while *TEC* represents the capability of the plant to convert the available water in aboveground biomass. According to Spearman's analysis, these two parameters were positively correlated to simulated fruit biomass, with similar strength ($\overline{SC}_{TEC}$ = 0.143, $\overline{SC}_{Rootini}$ = 0.139). The variability in the correlations of these parameters with fruit biomass (cv. TEC= 4%, cv. *Root$_{ini}$* = 3%) in the period of interest reflected the high year-to-year fluctuations of thermal conditions and cumulated precipitation in the study area (Table 2). Our results are in agreement with findings by Vanuytrecht et al. (2014), who demonstrated using the EFAST sensitivity analysis method that variations in the parameters related to root growth deeply affect maize yield in the AquaCrop model.

The MS resulted more responsive to the variation of the intercept value (*qRUE550*) rather than to the slope (*mRUE550*, 13th ranked) of the radiation use efficiency function, probably due to the ranges of values selected in this study. The *ShootNumber*, *PlantArea*, and *ProportionShadedArea* (8th, 9th, and 12th ranked, respectively), related to the representation of canopy characteristics and vine training systems, showed less importance in explaining fruit yield variability via their impact on the intercepted radiation rate. The *PlantArea* was the only parameter showing a negative correlation with fruit biomass, as it represents the inverse of planting density.

The *Tmax, Tmin* and *Topt* parameters were determinant in influencing fruit biomass variability, despite their low average correlation with this variable, modulating the impact of air temperatures (around flowering) on the fruit set process (data not shown).

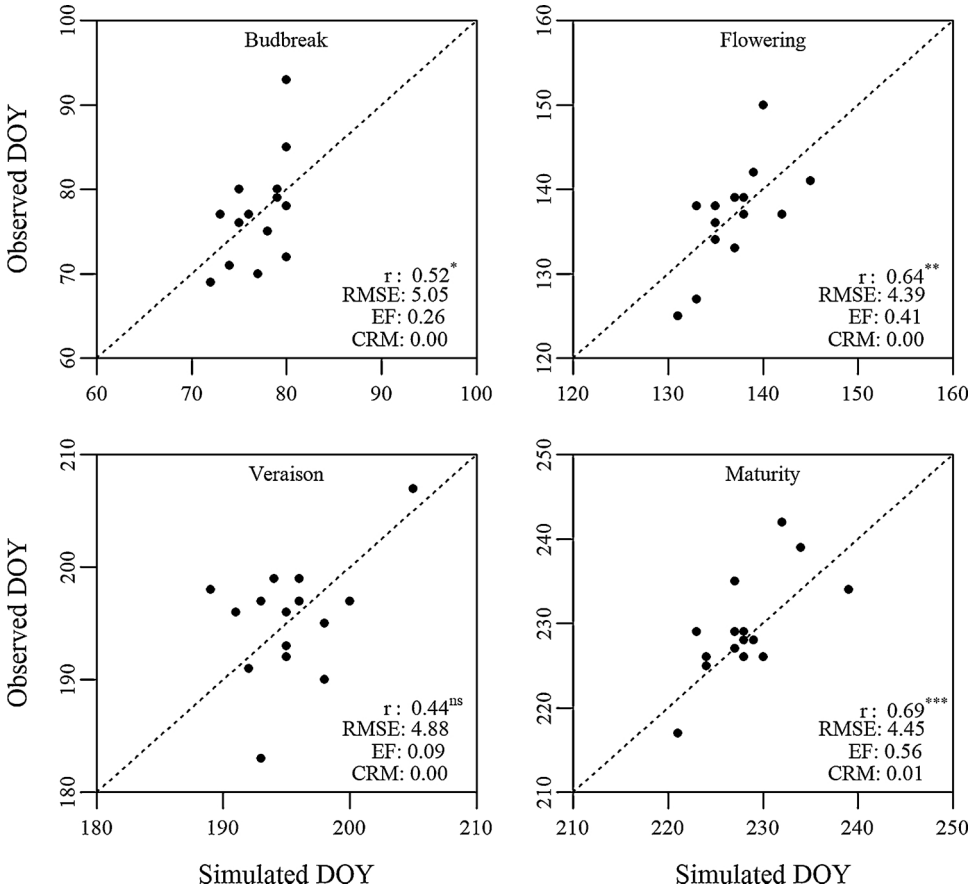

Fig. 5. Scatterplots presenting the comparison of simulated (X-axis) and observed (Y-axis) day of the year (DOY) referred to the main phenological phases of the Chardonnay grape variety (budbreak, flowering, veraison and maturity). Within each plot, the values of the root mean square error (RMSE), the coefficient of residual mass (CRM), the modelling efficiency (EF), the Pearson's coefficient (r), and the *F*-test significance of the correlation (ns, not significant relationship; *, $p < 0.05$; **, $p < 0.01$; ***, $p < 0.001$) are reported.

Fifteen parameters were included in the second step of the sensitivity analysis assessment (Sobol' Total Order; Fig. 4b). The ranking of the parameters most influencing fruit biomass variability after Sobol' sensitivity analysis reflected LHS results. The main difference between the two rankings was in the $Root_{ini}$ parameter, which gained relevance after Sobol' (4th ranked, $\overline{STL}_{Root_{ini}} = 0.06$), highlighting the large influence of root water uptake on fruit biomass, with a deep year-to-year variability (cv. 47%). The *SLAE* parameter ($\overline{STL}_{SLAE} = 0.521$, cv. 8%) consistently resulted as the most relevant, and even increased its relative importance with respect to *LAR1* ($\overline{STL}_{LAR1} = 0.176$, cv. 12%) and *HI* ($\overline{STL}_{HI} = 0.075$, cv. 31%), the latter confirming the high importance of partitioning rules on simulated output. The *Tmax* parameter (7th ranked, $\overline{STL}_{Tmax} = 0.02$, cv. 134%) presented the highest year-to-year variability in Sobol' Total Order index.

3.2. Field level application of the modelling solution

3.2.1. Phenological development

The comparison of observed and simulated day of the year corresponding to the main phenological phases (budbreak, flowering, veraison and maturity) of the Chardonnay variety is shown in Fig. 5, and the list of the calibrated parameter values is reported in the supplementary material, Table A.3. The modelling solution was more accurate in reproducing flowering (r = 0.64; RMSE = 4.39 days; EF = 0.41) and maturity (r = 0.69; RMSE = 4.45 days; EF = 0.56) stages, compared to budbreak (r = 0.52; RMSE = 5.05 days; EF = 0.26) and veraison (r = 0.44; RMSE = 4.88; EF = 0.09). Results were in line with Parker et al. (2011), who tested four phenology models (Spring Warming, Spring Warming from 1st of January, UniForc, UniChill) on several grape varieties on a large dataset. Parker et al. (2011) obtained a RMSE ranging from 5.4 to 6.1 days for flowering and from 8.0 to 10.2 days for veraison stage. Caffarra and Eccel (2010) obtained similar r (0.53–0.81) and RMSE (5.6–6.9) on budbreak phase of Chardonnay variety (data extracted from charts), using the same chilling-forcing model adopted here.

Although some authors (Fila et al., 2014; Parker et al., 2011) claimed that CF models did not lead to higher accuracy than pure forcing models in current climate, the adoption of a CF approach to simulate phenological development is considered adequate especially in warmer climate conditions (García de Cortázar-Atauri et al., 2009a). Indeed, high temperatures influence the release of the dormancy phase altering chilling-forcing requirements, leading to erratic budbreak estimations in simple forcing models. The worse performances in reproducing budbreak could be partially explained by the uncertainty of its detection in the field, as the duration of the 'greentip' (C for Baggiolini; 4 for Eichorn-Lorenz modified, 07 for extended BBCH-scales; Baggiolini, 1952; Eichhorn and Lorenz, 1977) period can be very short (Lavee and May, 1997). Also the occurrence of the veraison stage is subjected to large year-to-year variability, and presents spatial patterns within a vineyard, even among berries within each cluster (Coombe, 1992). Hence, the exact timing of colour change, especially in white varieties, is difficult to identify.

The calibrated base temperature for chilling accumulation was set to 1.8 °C, leading to the accomplishment of chilling requirements around the end of December (endo-dormancy). This agrees with experimental studies in which chilling requirement ranged from 0 to 10 °C (Botelho et al., 2007; Caffarra and Eccel, 2010; Dokoozlian, 1999; Pouget, 1963, 1968). After endo-dormancy period, the accumulation of forcing units until budbreak proceeded at a forcing rate of 0.23, with 15 °C as base temperature. This is in agreement with Chuine (2000), where the best temperature conditions for forcing units accumulation ranged from 10 °C to 25 °C in several arboreal trees. The half maximal development rate is reached at increasing air temperatures from flowering to maturity (inflection points from flowering to maturity are

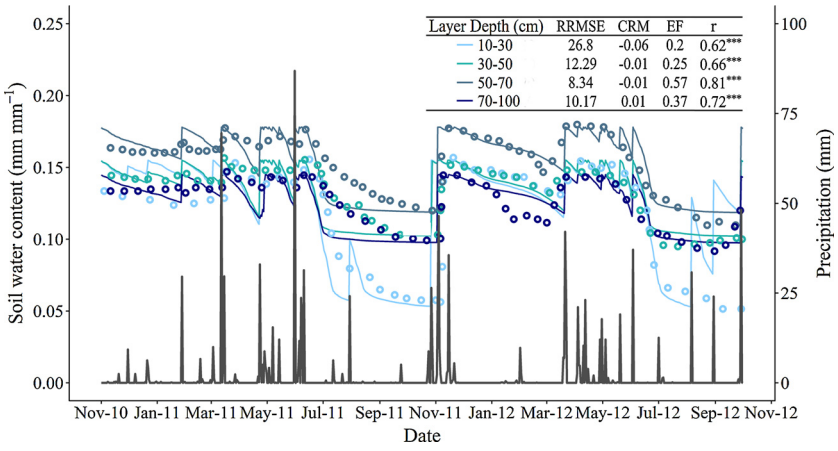
Layer Depth (cm) RRMSE CRM EF r
10-30 26.8 -0.06 0.2 0.62***
30-50 12.29 -0.01 0.25 0.66***
50-70 8.34 -0.01 0.57 0.81***
70-100 10.17 0.01 0.37 0.72***
Soil water content (mm mm−1)
Precipitation (mm)
Nov-10 Jan-11 Mar-11 May-11 Jul-11 Sep-11 Nov-11 Jan-12 Mar-12 May-12 Jul-12 Sep-12 Nov-12
Date

Fig. 6. Simulated (continuous lines) and observed (empty points) soil water content at different depths in two cropping seasons (2010–2012) in the experimental vineyard. Precipitation is reported on the secondary y-axis as grey line. The table at the top right of the figure resumes the performances of the modelling solution in the different layers, considering the relative root mean square error (RRMSE), the coefficient of residual mass (CRM), the modelling efficiency (EF), the Pearson's coefficient (r), and the *F*-test significance of the correlation (ns, not significant relationship; *, $p < 0.05$; **, $p < 0.01$; ***, $p < 0.001$).

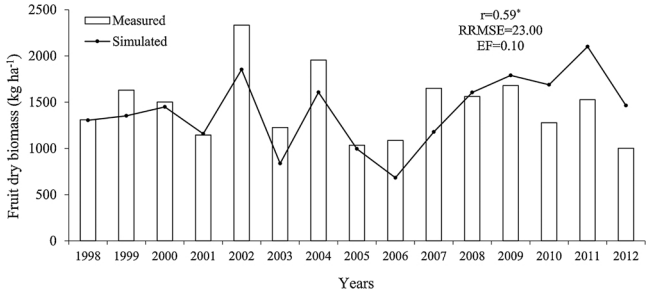

Fig. 7. Comparison of simulated (lines) and measured (histogram) fruit dry biomass (kg ha^{-1}) over the period 1998–2012. At the top right of the figure, the values of the relative root mean square error (RRMSE), the coefficient of residual mass (CRM), the modelling efficiency (EF), the Pearson's coefficient (r), and the *F*-test significance of the correlation (ns, not significant relationship; *, $p < 0.05$; **, $p < 0.01$; ***, $p < 0.001$) are reported.

respectively: ef = 9.43 °C, ev = 10.93 °C, em = 17.24 °C) as reported in Oliveira (1998) and Zapata et al. (2016), as well as the forcing unit accumulation rate (flowering rate df = 0.13; veraison rate dv = 0.40; maturity rate dm = 0.40). The calibrated threshold to reach veraison phase (57.31 FU) was higher than the flowering phase (38.47 FU), as in Caffarra and Eccel (2010). A lower thermal requirement was determined for maturity phase (30.73 FU), due to the higher forcing accumulation rate and the shorter length of the veraison-maturity period.

3.2.2. Soil water content

The comparison of simulated (lines) and measured (points) soil water content (SWC, mm mm^{-1}) at different depths in the experimental field is presented in Fig. 6, considering the data availability limited to November 2010-September 2012 (Ramos and Martínez-Casasnovas, 2014).

The 2011 cropping season was characterized by 86.3 mm of cumulated precipitation during bud break-flowering period, 184.6 mm in flowering-veraison - concentrated in few high intensity events - and 17.67 mm in the last part of the vine cycle. This determined a steep SWC decline in the whole profile in early June, with no recharge until the end of the cropping season. In 2012, larger precipitation events (217.8 mm) occurred during budbreak-flowering period. The corresponding measured and simulated SWC was higher, with full water availability in the whole profile until the beginning of July. Later in the season, very small precipitation events were recorded, thus determining a steep SWC decrease until harvest date.

The first soil layer (10–30 cm) presented a larger water holding capacity (field capacity = 0.16 mm mm^{-1}, wilting point = 0.05 mm mm^{-1}) than deeper layers. The modelling solution correctly reproduced SWC measurements, with RRMSE values ranging from acceptable (1st layer, 26.8%) to excellent performances (< 10%) in the whole soil profile (Jamieson et al., 1991). RRMSE values in the four soil layers are consistent with published simulation studies where SWC was simulated (Bregaglio et al., 2016; Constantin et al., 2015; Markewitz et al., 2010). The lower accuracy obtained in the surface soil layer is due to its sudden refill up to field capacity as a consequence of small precipitation events during simulation. Indeed, this layer was characterized by a systematic overestimation of SWC (CRM = -0.06), whereas no bias emerged in the deeper layers (-0.01 ≤ CRM ≤ 0.01). Our results agree with Molina-Herrera et al. (2016), where the r coefficient between observed and simulated SWC at 10 cm depth ranged from 0.28 to 0.79 in several agricultural sites. The EF was positive throughout the soil profile, proving the accuracy of the modelling solution in reproducing SWC, which decreased as a consequence of root water uptake during vegetative seasons. The r coefficient and EF are consistent with the results reported by Toumi et al. (2016) (r: 0.75-0.82; EF: -2.62-0.55) in which the soil water content (0–55 cm) is simulated considering the inputs of rainfall and irrigation under limited water conditions.

3.2.3. Fruit biomass

The comparison of measured and simulated fruit dry biomass (kg ha^{-1}) in the period 1998–2012 is shown in Fig. 7. The overall correlation was significant (r = 0.59, p < 0.05), and proved the capability of the modelling solution in reproducing the large year-to-year variability characterizing reference yield data.

The values of RRMSE (23%) and EF (0.1) supported the ability of the modelling solution in reproducing measured yields. No leaf area index (LAI) data were available in the reference dataset. Indeed, simulated LAI in 1998–2012 (data not shown) ranged from 0.76 to 1.19 m^2 m^{-2}, which agrees with Chacón et al. (2009) and Pérez et al. (2013), who measured it in rainfed Spanish vines trained with a similar number of buds per plant.

The modelling solution correctly simulated low yields in 2001, 2003, 2005, and 2006, which were characterized by high water deficit during the flowering-veraison period (Ramos and Martínez-Casasnovas, 2014; Table A.2). Conversely, high yields were simulated in the years 2002, 2004 and 2011, according to field measurements. The modelling solution tended to overestimate reference yield data in the period 2010-2012. A possible reason is the adoption of a fixed coefficient to convert fresh into dry fruit biomass. The alternation of wet-dry conditions could indeed have determined a variable berry water concentration, with the years 2011 and 2012 being characterized by a higher water deficit before harvest time. A specific case was represented by the year 2002, in which rainfall events occurred in close proximity with harvest, with an impact on annual grape production. It was demonstrated that the percentage of dry weight at harvest can vary according to soil water availability (Girona et al., 2009), with the high water stress around

harvest reducing both dry matter production (Reynolds et al., 2007) and berry water content (Garcia de Cortázar-Atauri et al., 2009b; Petrie et al., 2000).

The reference data-sets used for the calibration of our new modelling solution were collected out in a vine orchard at full production, therefore we did not demonstrate here the capability of the model in reproducing vine growth dynamics in the first years of establishment of a new orchard. In this case, a specific calibration of the parameters related to the initial number of shoots of a single vine and of the ones used to modulate the leaf area expansion and root depth will be needed, in order to initialize the simulation to reflect the targeted grapevine age.

4. Conclusions

The availability of grapevine simulators to be used as in-season supporting tools or in medium-long term forecasting activities is recognized as a priority by the community, given the paramount importance of this key cash crop worldwide. The research products which are presented and released with this paper are meant to contribute to this aim, providing a starting point to further extend their implementation and use. The fine granularity adopted in model development allows third parties to independently extend the UNIFI.GrapeML software library, and the availability of BioMA tools for code generation and model analysis facilitate the fulfillment of these objectives. The new modelling solution proved to be adequate in reproducing a reference field dataset containing phenological, soil water content and yield data, although its operational application for climate change assessments must be limited to the explored variety and study area. New models targeted to capture the effect of extreme events on phenological development and on the qualitative aspects of grape yield need to be tested/implemented, to give a comprehensive model representation of this complex cropping system.

Acknowledgments

This study received financial support from (i) the MODEXTREME project (MODelling vegetation response to EXTREMe Events, http://modextreme.org), which has received funding from the European Community's Seven Framework Programme-FP7 (KBBE.2013.1.4-09) under Grant Agreement No. 613817.2013-2016.

Appendix A. Supplementary data

Supplementary material related to this article can be found, in the online version, at doi: https://doi.org/10.1016/j.eja.2018.06.006.

References

Acutis, M., Confalonieri, R., 2006. Optimization algorithms for calibrating cropping systems simulation models. A case study with simplex-derived methods integrated in the WARM simulation environment. Riv. Ital. Agrometeorol. 11, 26–34.
Allison, L.E., 1965. Organic carbon. In: Black, C.A. (Ed.), Methods of Soil Analysis. Part 2. Chemical and Microbiological Properties. Am. Soc. Agron., pp. 1367–1379 Publ. 9.
Amir, J., Sinclair, T.R., 1991. A model of water limitation on spring wheat growth and yield. Field Crop. Res. 28, 59–69.
Asseng, S., Ewert, F., Rosenzweig, C., Jones, J.W., Hatfield, J.L., Ruane, A.C., Brisson, N., 2013. Uncertainty in simulating wheat yields under climate change. Nat. Clim. Change 3, 827–832. https://doi.org/10.1038/nclimate1916.
Baggiolini, M., 1952. Stades repères de l'abricotier. Rev. Romande Agric. Vitic. Arboric. 8, 28–29.
Bannayan, M., Crout, N., 1999. A stochastic modelling approach for real-time forecasting of winter wheat yield. Field Crop. Res. 62, 85–95. https://doi.org/10.1016/S0378-4290(99)00008-8.
Bellocchi, G., Rivington, M., Donatelli, M., Matthews, K., 2010. Validation of biophysical models: issues and methodologies. Agron. Sustain. Dev. 30, 109–130.
Bindi, M., Miglietta, F., Gozzini, B., Orlandini, S., Seghi, L., 1997a. A simple model for simulation of growth and development in grapevine (Vitis vinifera L.). II. Model validation. Vitis 36, 73–76.
Bindi, M., Miglietta, F., Gozzini, B., Orlandini, S., Seghi, L., 1997b. A simple model for simulation of growth and development in grapevine (Vitis vinifera L.). I. Model description. Vitis 36, 67–71.
Bindi, M., Fibbi, L., Lanini, M., Miglietta, F., 2001a. Free air CO2 enrichment (FACE) of grapevine (Vitis vinifera L.): I. Development and testing of the system for CO2 enrichment. Eur. J. Agron. 14, 135–143. https://doi.org/10.1016/S1161-0301(00)00092-7.
Bindi, M., Fibbi, L., Miglietta, F., 2001b. Free Air CO2 Enrichment (FACE) of grapevine (Vitis vinifera L.): II. Growth and quality of grape and wine in response to elevated CO2 concentrations. Eur. J. Agron. 14, 145–155. https://doi.org/10.1016/S1161-0301(00)00093-9.
Bindi, M., Bellesi, S., Orlandini, S., Fibbi, L., Moriondo, M., Sinclair, T., 2005. Influence of water deficit stress on leaf area development and transpiration of sangiovese grapevines grown in pots. Am. J. Enol. Vitic. 56 (1), 68–72.
Bock, A., Sparks, T.H., Estrella, N., Menzel, A., 2013. Climate-induced changes in grapevine yield and must sugar content in Franconia (Germany) between 1805 and 2010. PloS One 8 (7), e69015. https://doi.org/10.1371/journal.pone.0069015.
Bota, J., Stasyk, O., Flexas, J., Medrano, H., 2004. Effect of water stress on partitioning of 14 C-labelled photosynthates in Vitis vinifera. Funct. Plant Biol. 31, 697–708. https://doi.org/10.1071/FP03262.
Botelho, R.V., Pavanello, A.P., José, E., Pires, P., Terra, M.M., Marques, M., Müller, L., 2007. Effects of chilling and garlic extract on bud dormancy release in cabernet sauvignon grapevine cuttings. Am. J. Enol. Vitic. 58, 402–404.
Bregaglio, S., Donatelli, M., 2015. A set of software components for the simulation of plant airborne diseases. Environ. Model. Softw. 72, 426–444. https://doi.org/10.1016/j.envsoft.2015.05.011.
Bregaglio, S., Orlando, F., Forni, E., De Gregorio, T., Falzoi, S., Boni, C., Pisetta, M., Confalonieri, R., 2016. Development and evaluation of new modelling solutions to simulate hazelnut (Corylus avellana L.) growth and development. Ecol. Model. 329, 86–99. https://doi.org/10.1016/j.ecolmodel.2016.03.006.
Brun, Cellier, 1992. Les gelées de printemps dans les vignobles septentrionaux. Progrès Agricole et Viticole.
Caffarra, A., Eccel, E., 2010. Increasing the robustness of phenological models for Vitis vinifera cv. Chardonnay. Int. J. Biometeorol. 54, 255–267. https://doi.org/10.1007/s00484-009-0277-5.
Cappelli, G., Bregaglio, S., Romani, M., Feccia, S., Confalonieri, R., 2014. A software component implementing a library of models for the simulation of pre-harvest rice grain quality. Comput. Electron. Agric. 104, 18–24. https://doi.org/10.1016/j.compag.2014.03.002.
Chacón, J.L., García, E., Martínez, J., Romero, R., Gómez, S., 2009. Impact of the vine water status on the berry and seed phenolic composition of "Merlot" (Vitis vinifera L.) cultivated in a warm climate: consequence for the style of wine. Vitis - J. Grapevine Res. 48, 7–9.
Chuine, I., 2000. A unified model for budburst of trees. J. Theor. Biol. 207, 337–347. https://doi.org/10.1006/jtbi.2000.2178.
Confalonieri, R., Bellocchi, G., Bregaglio, S., Donatelli, M., Acutis, M., 2010. Comparison of sensitivity analysis techniques : a case study with the rice model WARM. Ecol. Model. 221, 1897–1906. https://doi.org/10.1016/j.ecolmodel.2010.04.021.
Constantin, J., Willaume, M., Murgue, C., Lacroix, B., Therond, O., 2015. The soil-crop models STICS and AqYield predict yield and soil water content for irrigated crops equally well with limited data. Agric. For. Meteorol. 206, 55–68. https://doi.org/10.1016/j.agrformet.2015.02.011.
Coombe, B.G., 1992. Research on development and ripening of the grape berry. Am. J. Enol. Vitic. 43, 101–110. https://doi.org/10.1111/j.1755-0238.2000.tb00171.x.
Costantini, E.A.C., Bucelli, P., 2014. Soil and Terroir, in: Soil Security for Ecosystem Management. Springer International Publishing, pp. 97–113. https://doi.org/10.1007/978-3-319-00699-4_6.
DAR, 2008. Mapa de Sòls (1:25.000) de l'àmbitgeogràfic de la Denominaciód'-OrigenPenedès. Vilafranca del Penedès-Lleida. DepartamentdAgricultura,Alimentació i Acció Rural, Generalitat de Catalunya.
Del Furia, L., Rizzoli, A., Arditi, R., 1995. Lakemaker: a general object-oriented software tool for modelling the eutrophication process in lakes. Environ. Softw. 10, 43–64. https://doi.org/10.1016/0266-9838(94)00016-Z.
Dokoozlian, N.K., 1999. Chilling temperature and duration interact on the budbreak of "Perlette" grapevine cuttings. HortScience 34, 1054–1056.
Donatelli, M., Van Evert, F.K., Di Guardo, A., Adam, M., Kansou, K., 2006. A component to simulate agricultural management. In: Voinov, A., Jakeman, A.J., Rizzoli, A.E. (Eds.), iEMSs Third Biannual Meeting: "Summit on Environmental Modelling and Software". International Environmental Modelling and Software Society, Burlington, Vermont.
Donatelli, M., Confalonieri, R., Cerrani, I., Fanchini, D., Acutis, M., Tarantola, S., Baruth, B., 2009. LUISA (Library User Interface for Sensitivity Analysis): a generic software component for sensitivity analysis of bio-physical models. 18th World IMACS Congress and MODSIM09 International Congress on Modelling and Simulation. Modelling and Simulation Society of Australia and New Zealand and International Association for Mathematics and Computers in Simulation. pp. 2377–2383.
Donatelli, M., Russell, G., Rizzoli, A.E., Acutis, M., Adam, M., Athanasiadis, I.N., Balderacchi, M., Bechini, L., Belhouchette, H., Bellocchi, G., 2010. A component-based framework for simulating agricultural production and externalities. Environmental and Agricultural Modelling. Springer, pp. 63–108.
Donatelli, M., Bregaglio, S., Confalonieri, R., De Mascellis, R., Acutis, M., 2014. A generic framework for evaluating hybrid models by reuse and composition - a case study on soil temperature simulation. Environ. Model. Softw. 62, 478–486. https://doi.org/10.1016/j.envsoft.2014.04.011.
Dos Santos, T.P., Lopes, C.M., Rodrigues, M.L., De Souza, C.R., Maroco, J.P., Pereira, J.S., Silva, J.R., Chaves, M.M., 2003. Partial rootzone drying: effects on growth and fruit quality of field-grown grapevines (Vitis vinifera). Funct. Plant Biol. 30, 663–671. https://doi.org/10.1071/FP02180.

Dry, P.R., Loveys, B.R., Düring, H., 2000. Partial drying of the rootzone of grape. II. Changes in the pattern of root development. Vitis 39, 9–12.
Duchêne, E., Schneider, C., 2005. Grapevine and climatic changes: a glance at the situation in Alsace. Agron. Sustain. Dev. 25 (1), 93–99. https://doi.org/10.1051/agro:2004057.
Dzotsi, K.A., Basso, B., Jones, J.W., 2013. Development, uncertainty and sensitivity analysis of the simple SALUS crop model in DSSAT. Ecol. Model. 260, 62–76. https://doi.org/10.1016/j.ecolmodel.2013.03.017.
Eichhorn, K.W., Lorenz, D.H., 1977. Phänologische Entwicklungsstadien der Rebe. Nachrichtenbl. Deut. Pflanzenschutz. 29, 119–120.
Ewart, A., Kliewer, W.M., 1977. Effects of controlled day and night temperatures and nitrogen on fruit-set, ovule fertility, and fruit composition of several wine grape cultivars. Am. J. Enol. Vitic. 28, 88–95.
FAOSTAT, 2016. http://www.fao.org/faostat/en/ (accessed 13 October 2017).
Farquhar, G.D., Caemmerer, S.V., 1982. Modelling of photosynthetic response to environmental conditions. Physiological Plant Ecology II. Springer, pp. 549–587.
Fila, G., Gardiman, M., Belvini, P., Meggio, F., Pitacco, A., 2014. A comparison of different modelling solutions for studying grapevine phenology under present and future climate scenarios. Agric. For. Meteorol. 195–196, 192–205. https://doi.org/10.1016/j.agrformet.2014.05.011.
Forrester, J.W., 1961. Industrial Dynamics. MIT Press, Cambridge, MA.
Fraga, H., García de Cortázar Atauri, I., Malheiro, A.C., Santos, J.A., 2016. Modelling climate change impacts on viticultural yield, phenology and stress conditions in Europe. Glob. Change Biol. 22 (11), 3774–3788.
Gao, X., Giorgi, F., 2008. Increased aridity in the Mediterranean region under greenhouse gas forcing estimated from high resolution simulations with a regional climate model. Glob. Planet. Change 62, 195–209. https://doi.org/10.1016/j.gloplacha.2008.02.002.
Garcia de Cortazar-Atauri, I., Brisson, N., Ollat, N., Jacquet, O., Payan, J.C., 2009b. Asynchronous dynamics of grapevine (Vitis Vinifera) maturation: experimental study for a modelling approach. J. Int. des Sci. la Vigne du Vin 43, 83–97.
García de Cortázar-Atauri, I., Brisson, N., Gaudillere, J.P., 2009a. Performance of several models for predicting budburst date of grapevine (Vitis vinifera L.). Int. J. Biometeorol. 53, 317–326. https://doi.org/10.1007/s00484-009-0217-4.
Gee, G.W., Bauder, J.W., 1986. Particle-Size Analysis, Methods of Soil Analysis: Part 1—Physical and Mineralogical Methods. Soil Science Society of America, American Society of Agronomy.
Girona, J., Marsal, J., Mata, M., Campo, J.D.E.L., Basile, B., 2009. Phenological sensitivity of berry growth and composition of Tempranillo grapevines (Vitis vinifera L.) to water stress. Aust. J. Grape Wine Res. 15, 268–277. https://doi.org/10.1111/j.1755-0238.2009.00059.x.
Green, I.R.A., Stephenson, D., 1986. Criteria for comparison of single event models. Hydrol. Sci. J. 31, 395–411. https://doi.org/10.1080/02626668609491056.
Greer, D.H., Weston, C., 2010. Heat stress affects flowering, berry growth, sugar accumulation and photosynthesis of Vitis vinifera cv. Semillon grapevines grown in a controlled environment. Funct. Plant Biol. 37, 206–214. https://doi.org/10.1071/FP09209.
Haeseler, C.W., Fleming, H.K., 1967. Response of Concord Grapevines to Various Controlled Day-Temperatures. The Pennsylvania State University Bulletin 739, USA, 739, 16. .
Hannah, L., Roehrdanz, P.R., Ikegami, M., Shepard, A.V., Shaw, M.R., Tabor, G., Zhi, L., Marquet, P.A., Hijmans, R.J., 2013. Climate change, wine, and conservation. Proc. Natl. Acad. Sci. 110 (17), 6907–6912. https://doi.org/10.1073/pnas.1210127110.
Hargreaves, G.H., Samani, Z.A., 1982. Estimating potential evapotranspiration. J. Irrig. Drain. Div. 108, 225–230.
Huglin, P., Schneider, C., 1998. In: Tec & Doc Lavoisier (Ed.), Biologie et écologie de la vigne, Paris.
IDESCAT, 2013. https://www.idescat.cat/?lang=es. (accessed 15 April 2018).
James, L.D., Burges, S.J., 1982. Selection, calibration, and testing of hydrologic models. In: Haan, C., Johnson, H., Brakensiek, D. (Eds.), Hydrologic Modeling of Small Watersheds. American Society of Agricultural Engineers, St. Joseph, Mich. USA, pp. 437–472.
Jamieson, P.D., Porter, J.R., Wilson, D.R., 1991. A test of computer simulation model ARC-WHEAT1 on wheat crops grown in New Zealand. Field Crops Res. 27, 337–350.
Jones, G.V., Davis, R.E., 2000. Climate influences on grapevine phenology, grape composition, and wine production and quality for Bordeaux, France. Am. J. Enol. Vitic. 51, 249–261.
Jones, G.V., White, M.A., Cooper, O.R., Storchmann, K., 2005. Climate change and global wine quality. Clim. Change 73, 319–343. https://doi.org/10.1007/s10584-005-4704-2.
Kliewer, W.M., 1977. Effect of high temperatures during the bloom-set period on fruit-set, ovule fertility, and berry growth of several grape cultivars. Am. J. Enol. Vitic. 28, 215–222.
Lavee, S., May, P., 1997. Dormancy of grapevine buds - facts and speculation. Aust. J. Grape Wine Res. 3, 31–46. https://doi.org/10.1111/j.1755-0238.1997.tb00114.x.
Lebon, E., Pellegrino, A., Louarn, G., Lecoeur, J., 2006. Branch development controls leaf area dynamics in grapevine (Vitis vinifera) growing in drying soil. Ann. Bot. 98, 175–185. https://doi.org/10.1093/aob/mcl085.
Leolini, L., Moriondo, M., Fila, G., Costafreda-Aumedes, S., Ferrise, R., Bindi, M., 2017. Late spring frost impacts on future grapevine distribution in Europe. Field Crops Res. https://doi.org/10.1016/j.fcr.2017.11.018.
Loague, K., Green, R.E., 1991. Statistical and graphical methods for evaluating solute transport models: overview and application. J. Contam. Hydrol. 7, 51–73. https://doi.org/10.1016/0169-7722(91)90038-3.
Markewitz, D., Devine, S., Davidson, E.A., Brando, P., Nepstad, D.C., 2010. Soil moisture depletion under simulated drought in the Amazon: impacts on deep root uptake. New Phytol. 187, 592–607. https://doi.org/10.1111/j.1469-8137.2010.03391.x.
McKay, M.D., Beckman, R.J., Conover, W.J., 1979. Comparison of three methods for selecting values of input variables in the analysis of output from a computer code. Technometrics 21, 239–245.
Molina-Herrera, S., Haas, E., Klatt, S., Kraus, D., Augustin, J., Magliulo, V., Tallec, T., Ceschia, E., Ammann, C., Loubet, B., Skiba, U., Jones, S., Brümmer, C., Butterbach-Bahl, K., Kiese, R., 2016. A modeling study on mitigation of N2O emissions and NO3 leaching at different agricultural sites across Europe using LandscapeDNDC. Sci. Total Environ. 553, 128–140. https://doi.org/10.1016/j.scitotenv.2015.12.099.
Molitor, D., Caffarra, A., Sinigoj, P., Pertot, I., Hoffmann, L., Junk, J., 2014. Late frost damage risk for viticulture under future climate conditions : a case study for the Luxembourgish winegrowing region. Aust. J. Grape Wine Res. 20, 160–168. https://doi.org/10.1111/ajgw.12059.
Monsi, M., Saeki, T., 1953. The light factor in plant communities and its significance for dry matter production. Jpn. J. Bot. 14 (1), 22–52.
Monteith, J.L., 1965. Evaporation and environment. Symp. Soc. Exp. Biol., vol. 19. pp. 205–223 p. 4.
Moriondo, M., Jones, G.V., Bois, B., Dibari, C., Ferrise, R., Trombi, G., Bindi, M., 2013. Projected shifts of wine regions in response to climate change. Clim. Change 119 (3–4), 825–839. https://doi.org/10.1007/s10584-013-0739-y.
Moriondo, M., Ferrise, R., Trombi, G., Brilli, L., Dibari, C., Bindi, M., 2015. Modelling olive trees and grapevines in a changing climate. Environ. Model. Softw. 72, 387–401. https://doi.org/10.1016/j.envsoft.2014.12.016.
Mullins, M.G., Bouquet, A., Williams, L.E., 1992. Biology of the Grapevine. Cambridge University Press, Great Britain.
Narciso, G., Ragni, P., Venturi, A., 1992. Agrometeorological Aspects of Crops in Italy, Spain and Greece: A Summary Review for Common and durum Wheat, Barley, Maize, Rice, Sugar Beet, Sunflower, Soya Bean, Rape, Potato, Tobacco, Cotton, Olive and Grape Crops. Commission of the European Communities.
Nelder, J.A., Mead, R., 1965. A simplex method for function minimization. Comput. J. 7, 308–313.
Nendel, C., Kersebaum, K.C., 2004. A simple model approach to simulate nitrogen dynamics in vineyard soils. Ecol. Model. 177, 1–15. https://doi.org/10.1016/j.ecolmodel.2004.01.014.
OIV, 2017. State of the Vitiviniculture World Market. (accessed 13 October 2017. http://www.oiv.int/public/medias/5479/oiv-en-bilan-2017.pdf.
Oliveira, M., 1998. Calculation of budbreak and flowering base temperatures for Vitis vinifera cv. Touriga Francesa in the Douro Region of Portugal. Am. J. Enol. Vitic. 49, 74–78.
Palmer, J.W., 1977. Diurnal light interception and a computer model of light interception by hedgerow apple orchards. J. Appl. Ecol. 14, 601–614.
Parker, A.K., De Cortázar-Atauri, I.G., Van Leeuwen, C., Chuine, I., 2011. General phenological model to characterise the timing of flowering and veraison of Vitis vinifera L. Aust. J. Grape Wine Res. 17, 206–216. https://doi.org/10.1111/j.1755-0238.2011.00140.x.
Pérez, D., Castel, J., Intrigliolo, D.S., Castel, J.R., 2013. Response of “Muscat of Alexandria” wine grapes to irrigation in eastern Spain. IX International Symposium on Grapevine Physiology and Biotechnology 343–350. https://doi.org/10.17660/ActaHortic.2017.1157.48.
Petrie, P.R., Trought, M.C.T., Howell, G.S., 2000. Fruit composition and ripening of Pinot Noir (Vitis vinifera L.) in relation to leaf area. Aust. J. Grape Wine Res. 6, 46–51.
Poni, S., Palliotti, A., Bernizzoni, F., 2006. Calibration and evaluation of a STELLA software- based daily CO 2 balance model in Vitis vinifera L. J. Am. Soc. Hortic. Sci. 131, 273–283.
Pouget, R., 1963. Recherches physiologiques sur le repos végétatif de la vigne (Vitis vinifera L.): la dormance des bourgeons et le mécanisme de sa disparition. Ann. Amélior. Plant. 13 (1), 1–247.
Pouget, R., 1968. Nouvelle conception du seuil de croissance chez la vigne. Vitis 7 (201–205), 201–205.
Ramos, M.C., Martínez-Casasnovas, J.A., 2014. Soil water variability and its influence on transpirable soil water fraction with two grape varieties under different rainfall regimes. Agric. Ecosyst. Environ. 185, 253–262. https://doi.org/10.1016/j.agee.2013.12.025.
Ramos, M.C., Jones, G.V., Martínez-Casasnovas, J.A., 2008. Structure and trends in climate parameters affecting winegrape production in northeast Spain. Clim. Res. 38, 1–15. https://doi.org/10.3354/crPAGE00759.
Reynolds, A.G., Lowrey, W.D., Tomek, L., Hakimi, J., de Savigny, C., 2007. Influence of irrigation on vine performance, fruit composition, and wine quality of Chardonnay in a cool, humid climate. Am. J. Enol. Vitic. 58, 217–228.
Ritchie, J.T., 1974. Atmospheric and soil water influences on the plant water balance. Agric. Meteorol. 14, 183–198. https://doi.org/10.1016/0002-1571(74)90018-1.
Ritchie, J.T., 1998. Soil water balance and plant water stress. Understanding Options for Agricultural Production. Springer, Netherlands, pp. 41–54.
Ritchie, J.T., Otter, S., 1984. CERES-Wheat: a user oriented wheat yield model. Preliminary documentation. United States Department of Agriculture. Agric. Res. Serv. ARS 38, 159–175.
Rötter, R.P., Carter, T.R., Olesen, J.E., Porter, J.R., 2011. Crop–climate models need an overhaul. Nat. Clim. Chang. 1, 175–177. https://doi.org/10.1038/nclimate1152.
Ruget, F., Brisson, N., Delecolle, R., Faivre, R., 2002. Sensitivity analysis of a crop simulation model, STICS, in order to choose the main parameters to be estimated. Agronomie 22, 133–158. https://doi.org/10.1051/agro.
Saltelli, a., Andres, T.H., Homma, T., 1995. Sensitivity analysis of model output. Performance of the iterated fractional factorial design method. Comput. Stat. Data Anal. 20, 387–407. https://doi.org/10.1016/0167-9473(95)92843-M.
Saltelli, A., Tarantola, S., Chan, K.P.-S., 1999. A quantitative model-independent method for global sensitivity analysis of model output. Technometrics 41, 39–56. https://doi.

org/10.1080/00401706.1999.10485594.
Seguin, G., 1986. "Terroirs" and pedology of wine growing. Experientia 42, 861–873.
Seguin, G., 1988. Ecosystems of the great red wines produced in the maritime climate of Bordeaux. In: Proceedings of the Symposium on Maritime Climate Winegrowing. Geneva, NY: Department of Horticultural Sciences, Cornell University, Geneva, NY, USA.
Soltani, A., Sinclair, T., 2012. Modeling Physiology of Crop Development, Growth and Yield. CAB International, Wallingford, UK pp. 366.
Stella, T., Frasso, N., Negrini, G., Bregaglio, S., Cappelli, G., Acutis, M., Confalonieri, R., 2014. Model simplification and development via reuse, sensitivity analysis and composition: a case study in crop modelling. Environ. Model. Softw. 59, 44–58. https://doi.org/10.1016/j.envsoft.2014.05.007.
Tang, Y., Reed, P., Van Werkhoven, K., Wagener, T., 2007. Advancing the identification and evaluation of distributed rainfall-runoff models using global sensitivity analysis. Water Resour. Res. 43, 1–14. https://doi.org/10.1029/2006WR005813.
Tanner, C.B., Sinclair, T.R., 1983. Efficient water use in crop production: research or re.search? In: Taylor, H.M., Jordan, W.R., Sinclair, T.R. (Eds.), Limitations to Efficient Water Use in Crop Production. American Society of Agronomy, Crop Science Society of America, and Soil Science Society of America, Madison, Wisconsin, pp. 1–27.
Therond, O., Hengsdijk, H., Casellas, E., Wallach, D., Adam, M., Belhouchette, H., Oomend, R., Russellf, G., Ewert, F., Bergez, J.E., Janssend, S., Wery, J., Van Ittersumd, M.K., 2011. Using a cropping system model at regional scale: Low-data approaches for crop management information and model calibration. Agric. Ecosyst. Environ. 142, 85–94. https://doi.org/10.1016/j.agee.2010.05.007.
Tomasi, D., Jones, G.V., Giust, M., Lovat, L., Gaiotti, F., 2011. Grapevine phenology and climate change: relationships and trends in the Veneto region of Italy for 1964–2009. Am. J. Enol. Vitic. 62, 329–339. https://doi.org/10.5344/ajev.2011.10108.
Toumi, J., Er-Raki, S., Ezzahar, J., Khabba, S., Jarlan, L., Chehbouni, A., 2016. Performance assessment of AquaCrop model for estimating evapotranspiration, soil water content and grain yield of winter wheat in Tensift Al Haouz (Morocco): application to irrigation management. Agric. Water Manage. 163, 219–235. https://doi.org/10.1016/j.agwat.2015.09.007.
Tukey, L.D., 1958. Effects of controlled temperatures following bloom on berry development of the Concord grape (Vitis labrusca). Proc. Am. Soc. Hortic. Sci. 71, 157–166.
Van Keulen, H., Seligman, N.G., 1987. Simulation of Water Use, Nitrogen Nutrition and Growth of a Spring Wheat Crop. Simulation Monograph, Wageningen. .
Van Leeuwen, C., Darriet, P., 2016. The impact of climate change on viticulture and wine quality. J. Wine Econ. 11 (1), 150–167. https://doi.org/10.1017/jwe.2015.21.
Van Leeuwen, C., Seguin, G., 1994. Incidences de l'alimentation en eau de la vigne, appréciée par l'état hydrique du feuillage, sur le développement de l'appareil végétatif et la maturation du raisin (Vitis vinifera variété Cabernet franc, Saint-Emilion, 1990). J. Int. Sci. Vigne Vin. 28, 81–110.
Vanuytrecht, E., Raes, D., Willems, P., 2014. Global sensitivity analysis of yield output from the water productivity model. Environ. Model. Softw. 51, 323–332. https://doi.org/10.1016/j.envsoft.2013.10.017.
Varella, H., Guérif, M., Buis, S., 2010. Global sensitivity analysis measures the quality of parameter estimation: the case of soil parameters and a crop model. Environ. Model. Softw. 25, 310–319. https://doi.org/10.1016/j.envsoft.2009.09.012.
Von Hoyningen-Huene, J., 1981. Die Interzeption des Niederschlags in landwirtschaftlichen Pflanzenbeständen. Arbeitsbericht Deutscher Verband für Wasserwirtschaft und Kulturbau. DVWK, Braunschweig.
Wang, X., He, X., Williams, J.R., Izaurralde, R.C., Atwood, J.D., 2005. Sensitivity and uncertainity analyses of crop yields and soil organic carbon simulated with EPIC. Am. Soc. Agric. Eng. 48 (3), 1041–1054. https://doi.org/10.13031/2013.18515.
Wang, J., Li, X., Lu, L., Fang, F., 2013. Parameter sensitivity analysis of crop growth models based on the extended fourier amplitude sensitivity test method. Environ. Model. Softw. 48, 171–182. https://doi.org/10.1016/j.envsoft.2013.06.007.
Williams, L.E., Ayars, J.E., 2005. Grapevine water use and the crop coefficient are linear functions of the shaded area measured beneath the canopy. Agric. For. Meteorol. 132, 201–211. https://doi.org/10.1016/j.agrformet.2005.07.010.
Williams, J.R., Jones, C.A., Kiniry, J.R., Spanel, D.A., 1989. The EPIC crop growth model. Trans. Am. Soc. Agric. Eng. 32, 497–511. https://doi.org/10.13031/2013.31032.
Zacharias, S., Heatwole, C.D., Coakley, C.W., 1996. Robust quantitative techniques for validating pesticide transport models. Trans. ASAE 39 (1), 47–54. https://doi.org/10.13031/2013.27479.
Zapata, D., Salazar0-Gutierrez, M., Chaves, B., Keller, M., Hoogenboom, G., 2016. Predicting key phenological stages for 17 grapevine cultivars (Vitis vinifera L.). Am. J. Enol. Vitic. ajev -2016. https://doi.org/10.5344/ajev.2016.15077.